Cluster magnetic fields from large-scale-structure and galaxy-cluster shocks

Mikhail V. Medvedev,[1] Luis O. Silva,[2] and Marc Kamionkowski[3]
[1]*Department of Physics and Astronomy, University of Kansas, KS 66045*
[2]*GoLP/Centro de Fisica de Plasmas, Instituto Superior Técnico, 1049-001 Lisboa, Portugal*
[3]*California Institute of Technology, Mail Code 130-33, Pasadena, CA 91125*

The origin of the micro-Gauss magnetic fields in galaxy clusters is one of the outstanding problem of modern cosmology. We have performed three-dimensional particle-in-cell simulations of the nonrelativistic Weibel instability in an electron-proton plasma, in conditions typical of cosmological shocks. These simulations indicate that cluster fields could have been produced by shocks propagating through the intergalactic medium during the formation of large-scale structure or by shocks within the cluster. The strengths of the shock-generated fields range from tens of nano-Gauss in the intercluster medium to a few micro-Gauss inside galaxy clusters.

PACS numbers: 98.65.-r, 95.30.Qd, 52.65.Rr, 52.35.Qz, 52.52.Tc

The origin of the micro-Gauss magnetic fields observed in galaxy clusters [1, 2, 3] poses one of the most intriguing problems in modern cosmology. The most common explanation invokes the amplification of seed or primordial fields by hydrodynamic turbulence that have been excited during the processes of large-scale-structure (LSS) formation. Although there are viable astrophysical mechanisms that can generate seed fields with $B \sim 10^{-16}$ Gauss or weaker [4, 5, 6, 7], recent cosmological simulations [8] show that structure formation can amplify the field by no more than a factor of 10^3. Hence, in order to explain the observed intergalactic field, one needs seed fields as strong as $B \sim 10^{-9}$ Gauss. Scenarios with galactic winds and quasar-driven outflows [9, 10] can provide fields of such strength, but they are rather localized. It is thus not clear whether they can explain entirely the origin of the intergalactic fields in galaxy clusters.

Here we show that magnetic fields can be produced by collisionless shocks in galaxy clusters and in the intercluster medium (ICM) during LSS formation. Cosmological N-body and hydrodynamic simulations of LSS formation [11, 12] have shown that shocks with Mach numbers up to $M \sim 100$ are ubiquitous on scales of few to few tens of megaparsecs. Theoretical analysis of non-magnetized collisionless shocks indicates that they can generate subequipartition fields [13, 14, 15]. We verify this prediction with state-of-the-art numerical simulations. We present here three-dimensional (3D) particle-in-cell (PIC) simulations of the *nonrelativistic* (with $v = 0.1c$) Weibel instability [16, 17] in an *electron-proton* (with $m_p/m_e = 100$) plasma, thus guaranteeing a clear separation of the relevant time scales. These simulations are computationally expensive and represent a significant advance over previous studies, which simulated relativistic shocks ($v \sim c$) in an electron-positron or low-mass-ratio electron-ion plasmas ($m_i/m_e \leq 16$) [18, 19, 20]. Note that a recently discussed possibility that cluster shocks may produce the magnetic fields seen in galaxy clusters [21] was based on the assumption that the results of relativistic simulations will also apply in the nonrelativistic regime. Our nonrelativistic simulations fully confirm theoretical predictions and indicate that LSS shocks can produce magnetic fields of strengths of tens of nano-Gauss to few micro-Gauss in the intergalactic medium (IGM) and ICM, respectively.

The mechanism of the field generation at shocks is rather simple [13, 14]. As a shock propagates into an ambient medium, it reflects (or scatters) a fraction of the incoming (in the shock frame) particles back into the upstream region which then form counter-propagating streams. Both groups of particles (ICM/IGM and reflected particles) have bulk velocities of order the shock velocity $v_{\rm sh}$; they can also have some thermal spread. Both protons and electrons form the streams, so both species participate in the instability [32]. One can consider each charged particle in these streams as an elementary current. Since like currents attract each other, it is energetically favorable for the elementary currents to merge into larger current filaments. This process is inhibited at scales smaller than the plasma skin depth, $\sim c/\omega_p$ (ω_p is the plasma frequency), by strong electrostatic repulsion of like charges. In contrast, on large scales, the currents are quasi-neutral because of Debye shielding in a plasma. Hence, the filaments and associated magnetic fields grow rapidly. The process stops when most of the particles become trapped in the produced fields and can no longer amplify the field. This happens when the particle Larmor radius $\rho_L = v_{\perp B}/\omega_c$ ($v_{\perp B}$ is the particle velocity component transverse to the local magnetic field, and $\omega_c = eB/mc$ is the cyclotron frequency) becomes comparable to (or less than) the characteristic correlation scale λ_B of the field, $\rho_L/\lambda_B \sim 1$. At this time, the particle distribution is effectively isotropized, and so $v_{\rm thermal} \sim v_{\perp B} \sim v_{\rm sh}$.

The anisotropy of the particle distribution near a shock can be parameterized as,

$$A = (\epsilon_\parallel - \epsilon_\perp)/\epsilon_{\rm tot} \simeq (M^2 - 1)/(M^2 + 1), \qquad (1)$$

where $\epsilon_\parallel \propto v_{\rm sh}^2$ is the energy of the particle along the shock propagation direction; $\epsilon_\perp \propto v_{\rm thermal}^2 \simeq c_s^2$ is the thermal energy in the plane of the shock; $\epsilon_{\rm tot} = \epsilon_\parallel + \epsilon_\perp$

is the total energy; c_s is the sound speed upstream; and the Mach number of the shock is $M = v_{\rm sh}/c_s$. For strong shocks, $M \gg 1$, the anisotropy parameter is close to unity, $A \sim 1$. At a shock, the bulk velocities of the electron and proton components are both comparable to the shock velocity. Hence, the protons dominate over the electrons in the overall energy budget, and the magnetic field generated by the electrons is negligible compared with that generated by the protons. The growth rate and the wavenumber of the fastest growing mode (which, in fact, sets the spatial correlation scale of the produced field) are $\gamma_B = A\,\omega_{p,p}(v_{\rm sh}/c)$ and $k_B = A\,\omega_{p,p}/c$, where $\omega_{p,p} = \left(4\pi e^2 n_p/m_p\right)^{1/2} \approx 1.32\times 10^3 n_p^{1/2}\ {\rm s}^{-1}$ is the proton plasma frequency, and n_p and m_p are the number density and the mass of the protons, respectively. (We use cgs units throughout, unless stated otherwise.) The kinetic calculation of the growth rate and the instability threshold have been examined elsewhere [22]. Order-of-magnitude estimates of the magnetic-field e-folding time and the field correlation length at strong shocks ($M \gg 1$) are readily obtained as

$$\tau_B \ \sim\ 1/\gamma_B \simeq 2\times 10^2\ v_{\rm sh,7}^{-1} n_{\rm ICM,-4}^{-1/2}\ {\rm s}, \qquad (2)$$

$$\lambda_B \ \sim\ 2\pi/k_B \simeq 10^{10}\ n_{\rm ICM,-4}^{-1/2}\ {\rm cm}, \qquad (3)$$

for a typical ICM proton density of $n_{\rm ICM} \sim 10^{-4}\ {\rm cm}^{-3}$ and a typical shock velocity $v_{\rm sh} \sim 10^7\ {\rm cm\ s}^{-1}$; as usual, we denote $n_{\rm ICM,-4} = n_{\rm ICM}/(10^{-4}\ {\rm cm}^{-3})$ and $v_{\rm sh,7} = v_{\rm sh}/(10^7\ {\rm cm\ s}^{-1})$. Since it takes $N \sim$ few $\times$ 10 e-foldings to produce strong fields, we can readily estimate the thickness of a region of the field growth as $\Delta \sim N\,\tau_B\,v_{\rm sh} \sim N\,\lambda_B$.

The saturation level of the magnetic field is estimated from $\lambda_B \sim \rho_L = v_{\rm sh}/\omega_{c,p}$, where $\omega_{c,p} = eB/m_p c \approx 9.58\times 10^3\,B\ {\rm s}^{-1}$ is the proton cyclotron frequency. In a multiple-species plasma, however, saturation occurs at equipartition with the lightest species [23]. To incorporate this, we introduce an efficiency factor η, which in the electron-proton plasma is of order m_e/m_p. Finally,

$$\epsilon_B = \frac{B^2/8\pi}{m_p n_p v_{\rm sh}^2/2} \simeq \frac{B^2}{8\pi p_{\rm sh}} \simeq A^2\eta \sim 10^{-3}, \qquad (4)$$

where $p_{\rm sh}$ is the gas pressure behind the shock, and the last estimate is for strong shocks, $A \sim 1$.

Although there is no doubt that magnetic fields are generated at shocks through the Weibel instability, it is not clear whether they survive sufficiently far downstream to produce longstanding magnetic fields. The concern arises from the fact that the wavelength of the fastest-growing mode in the linear Weibel-instability analysis is very small, $\lambda_B \sim 2\pi c/\omega_{p,p} \simeq 10^{10}$ cm for a typical ICM particle density of $n \sim 10^{-4}\ {\rm cm}^{-3}$. Therefore, it is possible that the extremely short spatial scales—i.e., sharp field gradients—can be rapidly destroyed by dissipation on a plasma time scale of $\tau_B \sim 10^2$ s. Should this happen, the fields would occupy only a very narrow region near the shock front and, thus, would not result in long-lived cluster fields. Recently, it has been shown [24], both theoretically and using relativistic PIC simulations that the correlation length of the magnetic field (and, hence, its gradient scale) grows rapidly with time, thus drastically reducing diffusive (Ohmic) dissipation. These results suggest that the magnetic fields produced should survive on cosmological times.

In general, it is far from clear that nonrelativistic shocks can generate fields in the way relativistic shocks do. In order to test this, we have performed a set of 3D and 2D PIC simulations [25, 26] using a state-of-the-art, massively-parallel, electromagnetic, fully-relativistic, 3D PIC code OSIRIS 2.0 [27]. In our PIC simulations, the initial conditions are taken to be two streams of electrons and ions moving with relative bulk velocity $v_{\rm sh}$, which in our simulations we take to be $0.1\,c$. The four "species" of particles (the upstream and downstream electrons and ions) is then each assigned a Maxwell-Boltzmann distribution of velocities about the bulk velocity. Our ions are "light protons," positively-charged particles with mass $m_{\rm ions} = 100\,m_e$, a mass ratio large enough to guarantee that the electron and ion time scales are clearly separated. All of our simulations have volumes of 128^3 cells, although the cell sizes differ.

We first ran four shorter-duration test simulations, three of them 3D and one 2D. In the first 3D run, the box size was $(25.6\ c/\omega_{p,e})^3$ (where $\omega_{p,e}$ is the electron plasma frequency), and there were 4 particles/species/cell. The second simulation differed from the first only in that the box size was $(12.8\ c/\omega_{p,e})^3$, and the third simulation differed from the first only in that it had 8 particles/species/cell. These test simulations showed that neither the box size, nor the number of particles per cell affect the results within the available computational resources. We also ran a 2D simulation with 1280^2 cells, i.e, with a box of size $(256.0\ c/\omega_{p,e})^2$, with periodic boundary conditions and 9 particles/cell/species in order to examine the dynamics of a similar system in the plane transverse to the bulk motion of the shocked plasma (the configuration is identical to that in simulations of Ref. [24]). Comparison between the 3D simulations and the 2D simulations do not show significant differences (e.g., in terms of the saturation level of the magnetic field), only revealing the limitations of the 2D simulation (the Weibel instability is stronger in 2D), and confirming that the transverse dimensions of the 3D simulation box are not strongly affecting the field dynamics on the time scales analyzed here.

We then ran very long 3D simulations of colliding plasma slabs, for four sets of plasma parameters. One of the plasma slabs describes a shocked high–Mach-number plasma ($M = 20$, $v_{\rm th,e\,shock}/c = 0.05$, with either $v_{\rm th,i\,shock}/c = 0.005$ or $v_{\rm th,i\,shock}/c = 0.0$) with bulk motion along the x_1 direction. The different ion ther-

mal velocities correspond to the two extreme cases of a strongly turbulent shock [28], where electrons and ions in the shocked plasma are thermalized by plasma turbulence and a laminar shock [29, 30]. The second plasma slab describes the IGM/ICM plasma with either cold electrons, $T_e = 0$, or hot electrons, $T_e = T_i \simeq 10\,\mathrm{eV}$, such that $v_{\mathrm{th,e\,IGM}}/c = 0.05$, $v_{\mathrm{th,i\,IGM}}/c = 0.005$. All four of these simulations used a box of size $(25.6\ c/\omega_{p,e})^3$. We found that the different physical parameters did not reveal any significant differences in the evolution of ϵ_B. Our present choice of simulation parameters is strongly limited by the time scales involved in the mechanisms described here, and it aims to illustrate the key features of the magnetic-field generation in conditions relevant for nonrelativistic collisionless shocks.

In fact, when examining the temporal evolution of ϵ_B measured in the 3D simulations (Figure 1), we observe the key role played by the ions, with most of the magnetic-field energy generated by the Weibel instability originating in the shocked ions. All the runs revealed $\epsilon_B \simeq 10^{-3}$. Note that the Weibel-field growth of the ions saturates at lower relative ϵ_B than for electrons $\epsilon_{B,i} \sim (m_e/m_i)^{1/2}\epsilon_{B,e}$, where for species $s = i, e$, $\epsilon_{B,s} = (B^2/8\pi)(m_s n_s v_{\mathrm{sh}}^2/2)^{-1}$. A strong thermalization between the electrons in the two slabs is achieved very early in time via the electron Weibel instability, but ion thermalization is not observed in our simulations. Other instabilities with longer time scales (e.g., the ion acoustic instability) will be responsible for this. These instabilities are not observed in our simulations since the simulation box is not large enough.

The time scale for energy transfer between the ions and the magnetic field is the time scale for the Weibel instability of the ions, longer than the electron Weibel instability by a factor of $(m_i/m_e)^{1/2}$, thus making its observation in numerical simulations very time consuming. The structure of the generated magnetic field depicted in Figure 2 shows the typical configuration of a Weibel-driven field, in 3D and in the 2D plane transverse to the bulk motion of the shocked plasma, surrounding the self-generated current filaments, which are already evolving to longer wavelengths.

We have demonstrated that magnetic fields are produced at nonrelativistic collisionless shocks and their strengths are comparable to that observed in clusters. It is thus natural to explain the observed fields by the Weibel instability. If so, then the magnetization of clusters should begin around the reionization epoch, at redshifts of $z \sim 10-20$, when the gas becomes highly ionized and particle collisions become rare and inefficient. Our studies reveal that the magnetic field grows to an energy density of roughly a tenth of a percent of the initial kinetic-energy density, and hence constitutes a similar fraction, $\epsilon_B \sim 10^{-3}$, of the thermal energy density of the shocked gas. The actual number depends on complicated nonlinear dynamics of the currents in the downstream region. This value of the equipartition parameter corresponds to a magnetic-field strength of order

$$B \sim 10^{-8}\ \epsilon_{B,-3}^{1/2}\, v_{\mathrm{sh},7}\, n_{\mathrm{ICM},-4}^{1/2}\ \mathrm{Gauss}. \tag{5}$$

These values correspond to tens of nano-Gauss in the ICM and a few micro-Gauss inside galaxy clusters, the latter in excellent agreement with observations.

The simulations presented here model a strong shock with Mach number, $M = 20$. Can a weak, $M \sim 1$, shock generate fields as well? 3D simulations of weak shocks are hardly possible at present. However, theoretical analysis of the Weibel instability shows that fields are generated when the shock velocity is larger than the thermal velocity of ICM/IGM particles by a factor of two or more; that is, when $M \gtrsim 2$. The exact number depends on the actual particle distribution at the shock.

LSS shocks can be observed via (i) synchrotron emission by the shock-accelerated electrons in the *in situ* generated magnetic fields; (ii) inverse-Compton scattering of cosmic microwave background photons by the shock-accelerated electrons; (iii) Sunyaev-Zeldovich effect on thermal electrons in the shocked medium downstream; and/or (iv) an abrupt change in the Faraday rotation measure across the shock. The shock front appears to be very thin and will likely be unresolved. Since no sign of proton thermalization is seen by the end of the simulations, $t \sim 500\,\omega_{p,p}$, we can put a constraint on the shock thickness,

$$\Delta_{\mathrm{sh}} > 10^{13}\ n_{\mathrm{ICM},-4}^{-1/2}\ \mathrm{cm}. \tag{6}$$

Our present analysis does not consider the evolution of the fields on cosmological time scales. Numerical simulations of this type are hardly possible within the next few years. Theoretical considerations suggest that inverse cascade should result in the rapid transfer of magnetic energy from small (shock) to large (cosmological) scales, thus leading to the long-term survival of the fields [24]. An alternative possibility, that other instabilities [31] present in plasma could destroy the field entirely, is unlikely because the time scales involved are long enough for dynamos driven by turbulence and sheared motions of gas in clusters to further amplify and preserve the shock-generated magnetic fields. A detailed study of these issues is highly important, yet extremely difficult and should be addressed in the future.

LOS acknowledges the help of Michael Marti in performing the simulations, M. Tzonfres, M. Marti, Profs. Ricardo Fonseca and Warren Mori for discussions. MK acknowledges useful discussions with X. Chen, E. Nakar, and M. Milosavljevic. The simulations were performed in the eXpp cluster at IST, Lisbon. The work of MVM has been supported by DoE grant DE-FG02-04ER54790, NASA grant NNG-04GM41G, and the GRF fund. The work of LOS was partially supported by FCT (Portugal) through grants PDCT/FP/FAT/50190/2003 and

POCI/FIS/55905/2004. MK was supported by DoE DE-FG03-92-ER40701 and NASA NNG05GF69G.

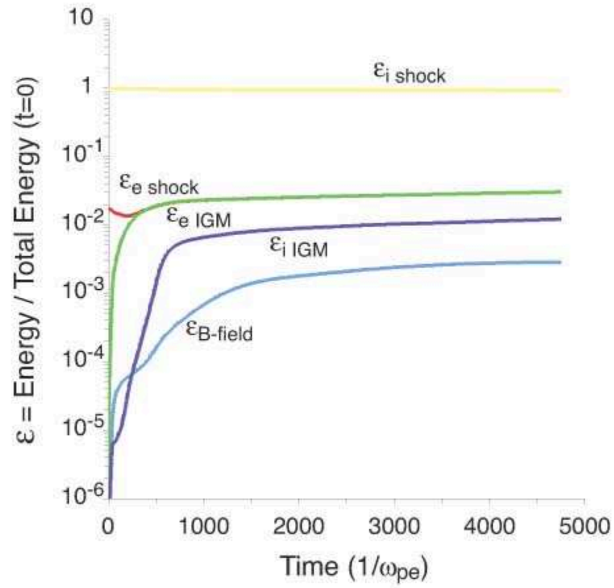

FIG. 1: The evolution of the magnetic field energy normalized by the total initial kinetic energy, ϵ_B, is shown with the light blue line. The energy in the magnetic field is predominantly associated with the field components parallel to the shock plane. For comparison, the similarly normalized energies for the four particle species are also shown.

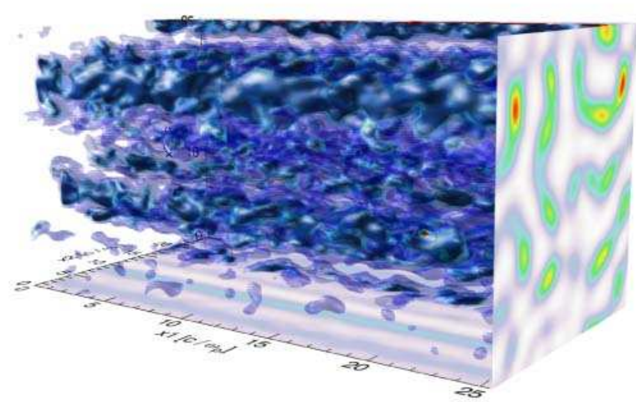

FIG. 2: Magnetic field energy density at $t = 2000/\omega_{p,e}$ ($\omega_{p,e}$ is the electron plasma frequency). The blue iso-surfaces correspond to a value of $\epsilon_B \simeq 8\times10^{-3}$. The projection in the x_2-x_3 plane (the shock plane) is the value of ϵ_B averaged along x_1 (the shock propagation direction) with red color corresponding to a peak value of $\epsilon_B \simeq 6\times10^{-2}$. The color scale in the projection plane is linear.

---

[1] G. B. Taylor, A. C. Fabian, and S. W. Allen Monthly Not. R. Astron. Soc. **334**, 769 (2002).
[2] A. Vikhlinin, M. Markevitch, and S. S. Murray, Astrophys. J. Lett. **549**, L47 (2001).
[3] C. Vogt, C. and T. A. Enßlin, Astron. & Astrophys. **412**, 373 (2003).
[4] L. Biermann, *Zs. Naturforschung A* **5**, 65 (1950).
[5] N. Y. Gnedin, A. Ferrara, and E. G. Zweibel, Astrophys. J. **539**, 505 (2000).
[6] E. R. Harrison, Monthly Not. R. Astron. Soc. , **147**, 279 (1970).
[7] H. Sicotte, Monthly Not. R. Astron. Soc. **287**, 1 (1997).
[8] M. Brüggen *et al.,* astro-ph/0508231 (2005).
[9] S. R. Furlanetto and A. Loeb, Astrophys. J. **556**, 619 (2001).
[10] O. D. Mirand, M. Opher, and R. Opher, Monthly Not. R. Astron. Soc. **301**, 547 (1998).
[11] F. Miniati *et al.,* Astrophys. J. **542**, 608 (2000).
[12] D. Ryu, H. Kang, E. Hallman, and T. W. Jones, Astrophys. J. **593**, 599 (2003).
[13] M. V. Medvedev and A. Loeb, Astrophys. J. **526**, 697 (1999).
[14] S. S. Moiseev and R. Z. Sagdeev, *J. Nucl. Energy C* **5**, 43 (1963).
[15] R. Schlickeiser and P. K. Shukla, Astrophys. J. Lett. **599**, L57 (2003).
[16] E. S. Weibel, Phys. Rev. Lett. bf 2, 83 (1959).
[17] B. D. Fried, *Phys. Fluids* **2**, 337 (1959).
[18] J. T. Frederiksen *et al.,* Astrophys. J. Lett. **608**, L13 (2004).
[19] K.-I. Nishikawa, *et al.,* Astrophys. J. **595**, 555 (2003).
[20] L. O. Silva, *et al.,* Astrophys. J. Lett. **596**, L121 (2003).
[21] Y. Fujita and T. N. Kato, astro-ph/0508589 (2005).
[22] M. Tzonfres *et al.*, Phys. Rev. Lett., submitted.
[23] J. Wiersma and A. Achterberg, Astron. & Astrophys. **428**, 365 (2004).
[24] M. V. Medvedev *et al.,* Astrophys. J. Lett. **618**, L75 (2005).
[25] C. K. Birdsall and A. B. Langdon, *Plasma Physics via Computer Simulation* (McGraw-Hill, New York, 1985).
[26] J. M. Dawson, *Rev. Mod. Phys.* **55**, 403 (1983).
[27] R. A. Fonseca *et al. Lecture Notes in Computer Science* **2331**, 342 (Springer-Verlag, Heidelberg, 2002)
[28] D. A. Tidman and N. A Krall, *Shock waves in collisionless plasmas* (Wiley, New York, 1971).
[29] D. W. Forslund and J. P. Freidberg, Phys. Rev. Lett. **27**, 1189 (1971).
[30] R. Z. Sagdeev, *Rev. Plasma Phys.* **4**, 23 (1966).
[31] M. Miloslavljevic and E. Nakar, astro-ph/0508464 (2005).
[32] Unlike the ultrarelativistic case, the growth rate of the electrostatic (Langmuir) instability may be greater than that of the Weibel instability. The electrostatic fields are predominantly longitudinal and scatter the particles in z-direction, not over the pitch angle. The overall anisotropy of the streams and, hence, the dynamics of the Weibel instability are not substantially affected. Therefore, we do not consider the Langmuir instability in this paper.